Journal of Physics: Conference Series

Fault Location of Hybrid Transmission Line Based on Zero Sequence Current and EMTR

To cite this article: LiQun Shang *et al* 2022 *J. Phys.: Conf. Ser.* **2310** 012008

Fault Location of Hybrid Transmission Line Based on Zero Sequence Current and EMTR

LiQun Shang[1a*], Peng Zang[1b*] , HaiYang Xu[1c]

[1]School of Electrical and Control Engineering, Xi'an University of Science and Technology, Xi'an 710699, Shaanxi Province, China

[a*] shanglq@xust.edu.cn, [b*] 604854564@qq.com, [c] 591186001@qq.com

Abstract: In order to better solve the problems of current cable-overhead hybrid lines that are affected by transition resistance, fault phase angle, and fault type in fault location, this paper proposes to use the zero-sequence current method to determine the large fault section first, and then according to the electromagnetic time reversal theory (EMTR) to realize the accurate location of faults in small sectionsa. A simulation model of a cable-overhead hybrid transmission line was established using ATP-EMTP, and the program was verified in MATLAB. The simulation results show that the method is not only not affected by the transition resistance and the phase angle of the fault, but also the type of fault has no effect on the results of the distance measurement, and it has higher positioning accuracy. With the allowable relative error, different types of faults can be accurately located.

1. introduction

The advantages and disadvantages of overhead lines and cable lines are different in terms of cost, maintenance, safety, stability, etc., so the combined use of overhead lines and cable lines can not only make the environment more beautiful, but also make the cost of erecting lines lower[1] . Therefore, the mixed use of overhead lines and cables is a common method in power construction. However, due to the different structures and parameters of overhead lines and cables, and frequent alternations in mixed use, the wave velocity in mixed lines is obviously discontinuous [2-5]. For a long time, the fault location of hybrid transmission lines has received extensive attention, and many articles on hybrid line location have been published at home and abroad [6-7]. Reference [8] proposes to apply the combination of traveling wave ranging method to hybrid transmission lines. Although it solves the defects affected by the length error of the power line and the synchronization deviation of the clocks of the two terminals, the process is cumbersome. Reference [9] judges the midpoint position of the time of failure according to the detection time, and then selects the corresponding direction to search and calculate successively, but its computational complexity will increase accordingly. Reference [10] uses wavelet analysis to detect faults, the fault is detected by the time-frequency characteristics of the reflected pulse, but the time-frequency analysis effect is easily affected by the selection of the small fundamental wave decomposition scale. The literature [11-13] uses the time discrimination method to detect the fault section, but its accuracy It is easily affected by the accuracy of the wave speed, and the fault section of the hybrid line in the complex environment cannot be detected directly by selecting the method of the wave speed according to the empirical value, and this method is not universal.

Aiming at the shortcomings of the above methods, a new hybrid line fault location method is proposed. First, by detecting the amplitude difference of the zero-sequence current in each section, it is determined whether the fault occurs in the overhead line section or the cable section, so as to realize the location of the large section; then, the electromagnetic time reversal theory is used to realize accurate distance measurement of small fault sections of hybrid transmission lines. The method only uses the amplitude of the zero-sequence current and does not involve the wave velocity, which effectively avoids the problem of ranging error caused by inaccurate wave velocity, and does not need to consider the complex traveling wave reflection problem in the hybrid line, which reduces the complexity of the algorithm. The electromagnetic time-reversal theory was first applied in acoustic research, and later, famous scholars tried to apply it to electromagnetic waves through derivation, using the time-reversal invariance of Maxwell's equations to achieve lightning localization, and achieved good results under ideal conditions [13]. In recent years, based on the basic theory of EMTR, the literature [14] applied the EMTR theory to the fault location of flexible HVDC transmission lines, and combined the wavelet technology in the information extraction. Reference [15] and Reference [16] proved the correctness of EMTR theory applied to lossless line fault location by calculation in the frequency domain, and proposed the section describes the basic process for locating faults; time reversal invariance, three different back propagation models are proposed: lossless model, lossy model and reverse loss model. Reference [17] applies EMTR theory to fault detection of different voltage levels of the same-pole double-circuit transmission line distance. Reference [18] applied the EMTR theory to the fault location of series-compensated transmission lines. It can be foreseen that the application of EMTR theory to the problem of fault location of cable-overhead line hybrid lines that are widely used at present has a very broad prospect.

2. Cable-overhead line hybrid line ranging principle

2.1 Fault segment judgment

To detect the fault of the hybrid transmission line, it is necessary to first determine which section the fault occurs in. Accurately judging the fault section is an important factor affecting the fault location accuracy of the hybrid transmission line. When the line fails, many transient signals, especially the zero-sequence current signal, will be generated. Before and after the fault occurs, the zero-sequence current value of the line will change abruptly. Therefore, by measuring the change of the zero-sequence current after the fault, the detection of the faulty section of the hybrid line can be achieved [19]. The equivalent network of cable-overhead line hybrid line is shown in Figure 1. MP is the overhead line segment, PN is the cable segment, and the fault occurs in the PN segment. A and B are the midpoints of the MP segment and the PN segment, respectively, A and B four positions are respectively installed with signal detection devices. When a fault occurs, it is equivalent to generating a fault voltage of Uf at the fault point. Due to the action of the fault voltage, the fault point will generate a fault traveling wave and propagate from the fault point to both ends of the line. At the detection points M and P on the same side of the fault point, the relationship between thezero-sequencecurrent is:

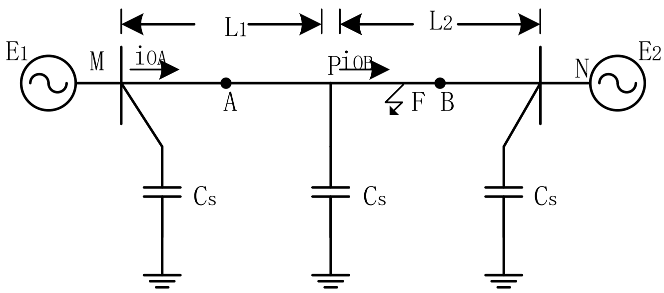

Fig． 1 Hybrid line equivalent network

$$i_{OM} = i_{OP} + i_{Cs} \tag{1}$$

In the formula: i_{OM} and i_{OP} are the zero-sequence currents flowing through M and P; i_{Cs} is the distributed capacitance current. In order to ensure the safety of power supply of high-voltage lines and reduce the risk of electric shock, capacitor current compensation is generally set on the line. Therefore, the capacitance current flowing through the adjacent points M and P is usually very small, which makes the zero-sequence current amplitudes of points M and P roughly equal. However, the zero-sequence current flowing through points P and N is affected by the line parameters (especially impedance parameters) on both sides, resulting in a relatively large difference in the magnitude of the zero-sequence current flowing through points P and N. To this end, a method for detecting the faulted section is proposed by using the difference in the amplitude of the zero-sequence current generated after the fault. Relative entropy is a common method used in engineering to compare the difference between two probability distributions. According to the principle of relative entropy, the zero-sequence current amplitude difference of the fault section in the hybrid line can be defined as:

$$P_k = \frac{\left|I_k\left(\ln I_k - \ln I_{k+1}\right)\right| + \left|I_k\left(\ln I_{k+1} - \ln I_k\right)\right|}{\sum\left(\left|I_k\left(\ln I_k - \ln I_{k+1}\right)\right| + \left|I_k\left(\ln I_{k+1} - \ln I_k\right)\right|\right)} \tag{2}$$

In the formula: k is the number of sections of the hybrid line; I_k is the zero-sequence current amplitude of each section.

$$I_k = \sqrt{\frac{1}{n}\sum_{k=1}^{n} i_0^2\left(k\right)} \tag{3}$$

The magnitude difference of the zero-sequence current reflects the change degree of the zero-sequence current at the beginning and end of each section of the line at the time of the fault, and the calculation result is in [0, 1]. When the fault detection point is located on the same side of the fault point, the smaller the change of the zero-sequence current at both ends of the interval line, the smaller the difference PK of the zero-sequence current amplitude (the minimum value can be 0). On the contrary, the greater the change of the zero-sequence current at both ends of the segmented line, the greater the difference PK of the zero-sequence current amplitude (the maximum value is 1). As shown in Figure 1, when a fault occurs in the PN section, the zero-sequence currents of the detection points P and N on the opposite side of the fault point vary greatly, and the corresponding zero-sequence current amplitude difference is close to 1, so the PN section belongs to the fault section, and the corresponding zero-sequence currents The magnitude difference of the current is close to 0, so the MP section is a non-fault section. In this way, the faulty section can be detected, and then the EMTR ranging method can be used to further determine the faulty section, narrow the scope of the faulty section, and accurately realize the fault location of the hybrid line [20-21].

2.2 EMTR theory of fault location

2.2.1 The theoretical basis of EMTR

The core strategy of EMTR theory is to reverse the time of the measured signal (Time Reversal, TR), that is, to change the direction of the current signal time axis t →-t [13]. Take the voltage fluctuation equation (4) of a lossless transmission line (abbreviated as lossless line) as an example

$$\frac{\partial^2 u(z,t)}{\partial z^2} - LC\frac{\partial^2 u(z,t)}{\partial t^2} = 0 \tag{4}$$

Time reversal of Equation (4), Equation (5) can be obtained

$$\frac{\partial^2 u(z,-t)}{\partial t^2} - LC\frac{\partial^2 u(z,-t)}{\partial t^2} = 0 \tag{5}$$

If u(z, t) is one of the solutions to the equation, then u(z, -t) is also a solution to the equation, indicating that the wave equation is invariant under time reversal. In actual ranging, the measured signal is only a small time period. Set the intercepted time period as T, and perform time reversal on the signal, that is, t→T-t.

For example, in space lightning localization, the electric field observed everywhere can be expressed by the following formula

$$\overrightarrow{E_n}(t)=\vec{E}(\overrightarrow{r_n},t)=\frac{\vec{\phi}\left(t-\frac{\left\|\overrightarrow{r_n}-\overrightarrow{r_s}\right\|}{c}\right)}{\left\|\overrightarrow{r_n}-\overrightarrow{r_s}\right\|} \tag{6}$$

where $\vec{\phi}(\mathrm{t})$ is the potential function, and its specific expression depends on the discharge current at the lightning position; c is the propagation velocity of the electric field in space; $\overrightarrow{r_n}$ is the position vector of the observation point n in space, $\overrightarrow{r_s}$ is the position vector of lightning in space. After time-reversing the above formula, we can get

$$\overrightarrow{E_n^{TR}}(t)=\overrightarrow{E_n}(T-t)=\frac{\vec{\phi}\left[T-\left(t-\frac{\left\|\overrightarrow{r_n}-\overrightarrow{r_s}\right\|}{c}\right)\right]}{\left\|\overrightarrow{r_n}-\overrightarrow{r_s}\right\|} \tag{7}$$

$\overrightarrow{E_n^{TR}}(t)$is the electric field after time-reversal at each observation point.

2.2.2 EMTR Theory Proof

Taking a single-phase single non-destructive conductor as an example, a simple proof of the EMTR theory is carried out, and the detailed proof can be found in reference [15].As shown in Figure 2(a), for a line of length S, the inductance and capacitance per unit length are L and C, respectively. When a fault occurs at the line X_F, its voltage to ground is u_F, and the distances between the fault point and the observation points M and N set at the left and right terminals of the line are l_z and l_y。 respectively. If the refraction and reflection are not considered, the current flowing from the fault point to the left and right ends of the line is the same,i_F。

Because the line has no loss, the currents i_M and i_N recorded at the observation points at the left and right ends of the line are as follows:

$$i_M=i_F(t-l_z/v) \tag{8}$$

$$i_N=i_F(t-l_y/v) \tag{9}$$

Where v is the traveling wave velocity, which is $1/\sqrt{LC}$. Time reversal of i_M and i_N can get ${i_M}^{TR}$ and ${i_N}^{TR}$, Assuming that the transient signals of $i_M(t)$and$i_N(t)$ are recorded within the time window T, considering the specific application, a time delay T is added to keep the time positive during the study period, namely:

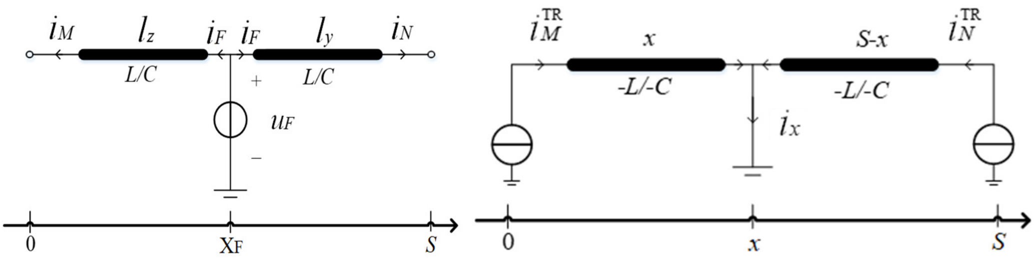

(a) Schematic diagram of the system after failure (b) Time-reversed current powers the mirror line

Fig．2 EMTR theory proof of lossless line

$$i_M^{TR}(t)=i_M(T-t)=i_F[T-(t-\frac{l_z}{v})] \tag{10}$$

$$i_N^{TR}(t)=i_N(T-t)=i_F[T-(t-\frac{l_y}{v})] \tag{11}$$

Set the line inductance and capacitance to -L and -C to construct its mirror image line, as shown in Figure 2(b), and the wave speed is unchanged at this time. Then connect ${i_M}^{TR}(t)$ and ${i_N}^{TR}(t)$ as current sources to the left and right ends of the mirror line to supply power. Assuming that a metallic ground fault occurs at any length x from the end of the line M, regardless of refraction, the current i_x at the fault point x is ${i_M}^{TR}(t)$ and ${i_N}^{TR}(t)$, which is added after a delay。

$$\begin{aligned} i_x &= i_M^{TR}(t-\frac{x}{v}) + i_N^{TR}[t-\frac{(S-x)}{v}] \\ &= i_F(T-t+\frac{l_z-x}{v}) + i_F(T-t-\frac{l_z-x}{v}) \end{aligned} \tag{12}$$

It can be known from equation (12) that in the T period, if and only if the fault point is assumed to be coincident with the real fault point, the current of the fault point obtains the maximum value.

3. Steps for fault location of hybrid lines

The failure of the line is basically the propagation of the electromagnetic field in the line, which can be reflected by the changes of the voltage and current around the line. Considering the direction of the electromagnetic field, the EMTR method is used to reverse the time of the electric field generated by the fault current, and then the location of the fault in the constructed circuit can be known by calculation. After the line fails, it is necessary to filter the fault current signal measured by the device to extract useful current components. The wavelet function can represent the signal characteristics of different scales and does not need to directly deal with a large number of wavelet coefficients [22], so this paper selects the wavelet function to analyze the filtered fault signal. Figure 3 shows the overall fault location algorithm flow.

Step1：After the fault occurs, record two fault currents in the line, denoted as $i_{M(t)}/i_{P(t)}$, and decouple through phase-mode transformation

Step2：The wavelet function is selected to decompose the decoupled transient to obtain the current abrupt change; this paper selects the "cD1" layer component after wavelet decomposition.

Step3：According to the extracted zero-sequence current component amplitude difference, determine the large section where the fault occurs.

Step4：Set the selected waveform time interval as T, the current abrupt change is reversed during this time interval, and the M-side inversion current is i_{Mf}(T-t), and the P-side inversion current is i_{Pf}(T-t).

Step5：Faults are assumed at various locations in the hybrid line. Let the total length of the line and the fault distance (the distance between the fault point F and the M-side busbar) be l and lz respectively. Carry out the time shift of t1=l/v and t2=(l-lz)/v respectively for the current abrupt changes after the inversion of the M side and the P side, and superimpose the two current sudden changes after the change, as shown in formula (13) shown

$$i_{l_z} = i_{Mf}(T-t-t_1) + i_{Nf}(T-t_2) \tag{13}$$

Step6：Use formula (14) to calculate the rms value of the current at the assumed fault location, and the distance corresponding to the maximum rms value is the fault distance.

$$\left| i_{l_z} \right| = \sqrt{\left[\sum_{n=1}^{\frac{T}{f_s}} i_{l_z}(nf_s) \right] / (\frac{T}{f_s})} \tag{14}$$

In the formula: f_s is the sampling rate of the wave recording device.

4. Simulation Analysis of Hybrid Line Fault

4.1 Simulation model and parameters

In order to verify the effectiveness of the proposed fault location method, a cable-overhead line hybrid line simulation model is established in the ATPDraw platform, and the schematic diagram of the model is shown in Figure 4. Among them, the M side power supply voltage $E_M=220\angle 0^{\circ}$, the M power supply impedance is:$Z_1=0.54+j18.25\Omega$ 、 $Z_0=1.58+j54\Omega$; the N power supply impedance is:$Z_1=0.33+j90\Omega$、$Z_0=0.9+j133\Omega$; When building the model in , the Bergeron model is used for the overhead lines and cable lines of the transmission line, and the lines are evenly transposed. In the figure, MP is an overhead line with a length of 200km. In ATP-EMTP The parameter settings are shown in Table 1, PN is the cable line, and the cable is laid out with a single-core coaxial cable with a length of 100km. and the parameter settings in ATP-EMTP are shown in Table 2.

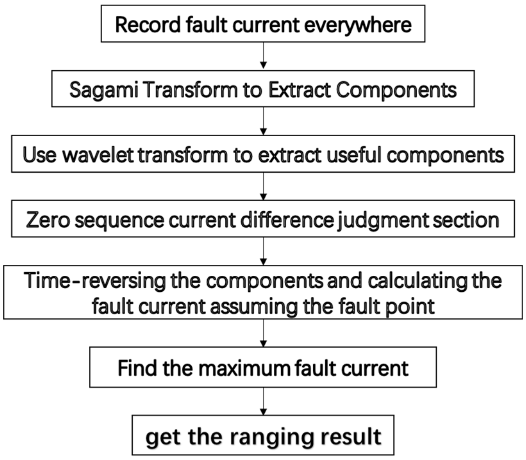

Fig． 3 Flow chart of the ranging algorithm

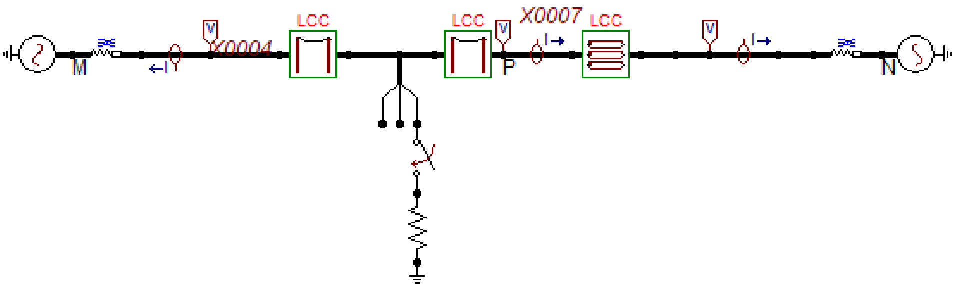

Fig． 4 Schematic diagram of mixed line simulation model

Tab． 1 220kV hybrid line overhead line parameters

Ph.no	Rout [cm]	Resis [ohm/km]	Horiz [m]	Vtower [m]	Vmid [m]	Separ [cm]	Alpha [deg]	NB
1	1.33	0.04	0	20.5	13.1	45	90	2
2	1.33	0.04	3	22.5	15.1	45	90	2
3	1.33	0.04	-3	20.5	13.1	45	90	2
0	0.55	0.2654	4	26	20.6	0	0	0
0	0.55	0.2654	-4	26	20.6	0	0	0

Note: 1, 2 and 3 in the table correspond to three-phase lines respectively, O is the lightning protection line; the central axis is OO' in the structure diagram, the left side is negative, and the right side is positive.

Tab. 2 220kV hybrid line cable parameters

Ph.no	Rin [m]	Rout [m]	Rho [ohm/km]	Horiz [m]	d [m]
1	0.0105	0.0178	0.0183	-0.25	-1.045
2	0.0105	0.0178	0.0183	0	-1.045
3	0.0105	0.0178	0.0183	0.25	-1.045

4.2 Simulation process

Simulate the fault of A-phase grounding at the distance of 60km from the M terminal of the overhead-cable hybrid line powered by the 220kV power supply at both ends. In the ATP Setting, set the simulation time length Tmax=0.2s; the sampling frequency is 1MHz, so in the simulation time A total of 4000 points were sampled; the moment when the fault occurred was 0.1s; the grounding resistance was 10Ω.

Record the current data in the time period of 0.098-0.102s. Decoupling the recorded current data, the 2-mode current component on the M side can be obtained as shown in Figure 5(a), and the 2-mode current component on the P side as shown in Figure 5(b).

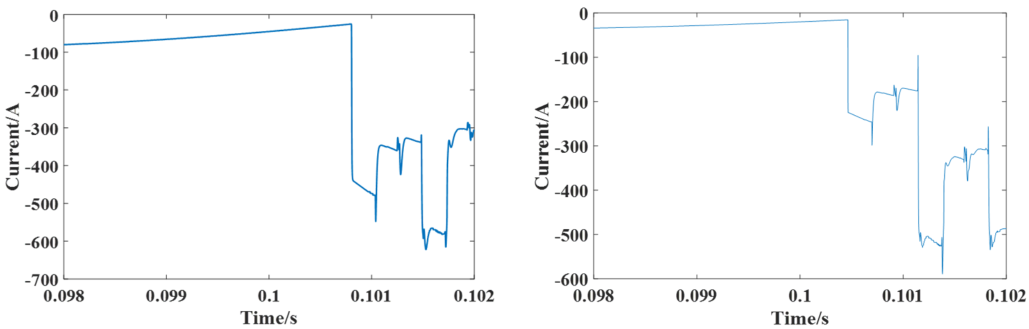

(a) 2-mode current components on the M side (b) 2-mode current components on the P side

Fig.5 Current components on both sides

The decoupled M-side and N-side in-direction 2-mode current components are decomposed by wavelet function using the 'db2' wavelet function. Figure 6(a) is the wavelet decomposition value of the M-side current, and Figure 6(b) is the M-side current wavelet decomposition value after time reversal. Figure 7(a) is the wavelet decomposition value of the P-side current, and Figure 7(b) is the P-side current wavelet decomposition value after time reversal.

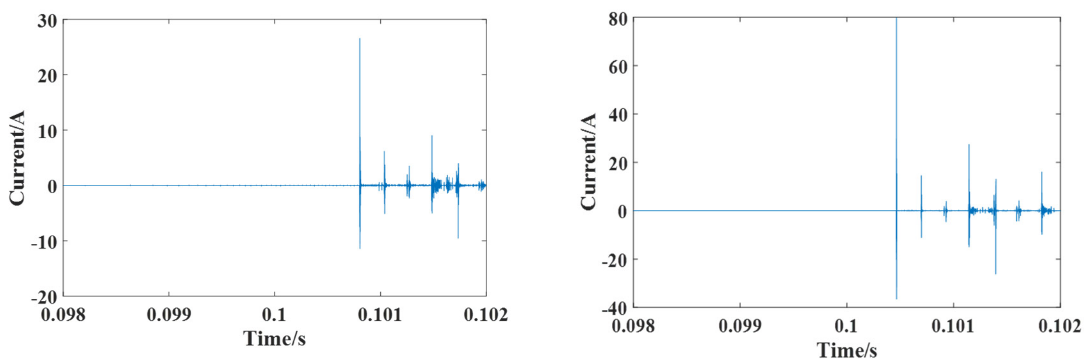

(a) Current wavelet decomposition value of M side (b) P side current wavelet decomposition value

Fig. 6 Wavelet decomposition values of currents on both sides

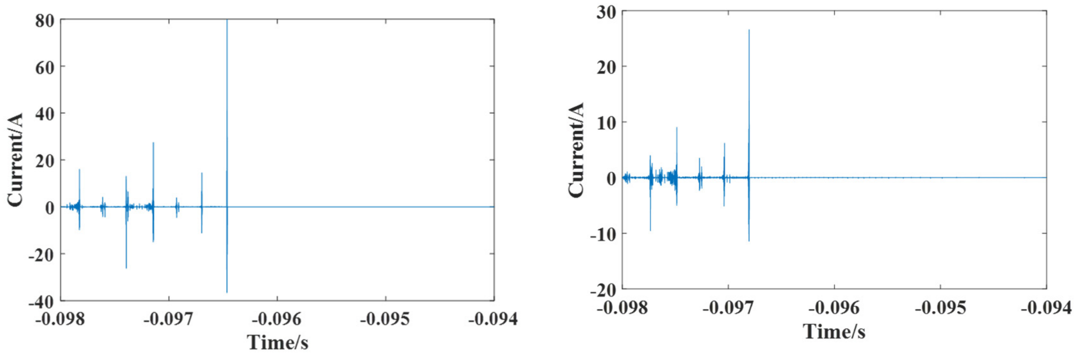

(a) Current decomposition value of M side after inversion (b) P-side current decomposition value after inversion

Fig.7 Wavelet decomposition value after time reversal

Assuming that a fault occurs at 60km of the line, the RMS current at the fault location is calculated according to Equation (14). Figure 8 shows the hypothetical RMS current along the line. It is found that the RMS current takes the maximum value at 61.6km, so the actual fault distance is 61.6km.

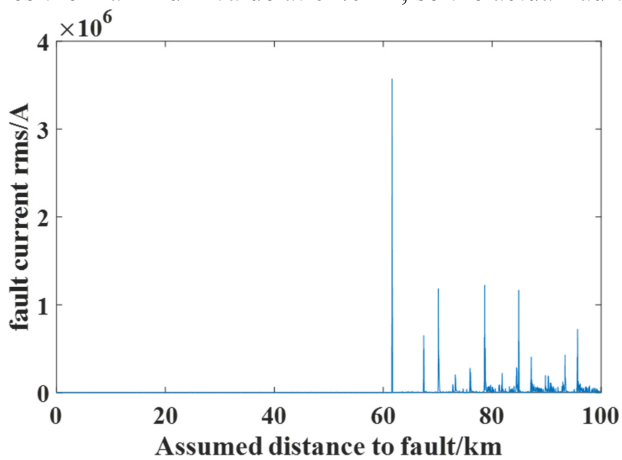

Fig. 8 The effective value of the fault current at a distance of 60km from the M side

5 Simulation verification of different faults

5.1 Effects of different fault types

In order to verify the feasibility of the above fault location method, different types of faults are simulated in this paper for verification, and the simulation results are shown in Table 3. The calculation method of the relative error (δ) of ranging is shown in formula (15).

$$\delta = \left| \frac{x_a - x_b}{x} \right| \times 100\% \qquad (15)$$

In the formula: x_a is the calculated fault distance; x_b is the actual fault distance; x is the full length of the line.

Tab. 3 Ranging results of different fault types

Fault type	actual fault distance /km	Ranging results /km		
		ground resistance 10	ground resistance 50	ground resistance 100
single-phase groundA-G	60	61.4	61.4	61.4
	120	121.2	121.2	121.2
	240	239.6	239.6	239.6

	60	61.6	61.6	61.6
Phase-to-phase short circuitAB	120	118.7	118.7	118.7
	240	241.5	241.5	241.5
	60	58.3	58.3	58.3
Phase-to-phase short-circuit to groundABG	120	121.8	121.8	121.8
	240	241.1	241.1	241.1
	60	59.0	59.0	59.0
Three-phase short circuitABC	120	118.8	118.8	118.8
	240	242.0	242.0	242.0

It can be seen from Table 3 that the fault type, fault location and transition resistance have no effect on the ranging results, and the ranging accuracy is less than 0.60%.

5.2 Effect of Fault Phase Angle

Table 4 shows the ranging results on both sides of the power supply under different initial phase angles and included angles. The transition resistance is set to 10Ω. Assume that the fault distance is 50km.

Tab. 4 Single-phase ground fault location results under different initial phase angles of the power supplies on both sides

Left and right power initial phase angle (°)	actual fault distance /km	Ranging results /km	Ranging relative error（%）
0-0	50	50．7	0.23
45-45	50	50．7	0.23
90-90	50	50．7	0.23
0-30	50	50．7	0.23
30-0	50	50．7	0.23
45-75	50	50．7	0.23
75-45	50	50．7	0.23
90-120	50	50．7	0.23
120-90	50	50．7	0.23

It can be seen from Table 4 that the lead lag on both sides of the power supply and different initial phase angles have no effect on the ranging results, and the accuracy of the ranging results is 0.23%.

It can be seen from Table 3 and Table 4 that the distance measurement results obtained by this algorithm are not affected when the fault type, fault distance, fault phase angle and transition resistance are different, and the accuracy of the distance measurement results is less than 0.60%.

5.3 Influence of sampling frequency

Because the different sampling frequency may also cause great errors in the ranging results, the sampling frequency is changed to verify the applicability of the method. The fault type is set as a single-phase-to-ground fault, and it is assumed that the fault occurs at 150km of the line. Table 5 presents the simulation results.

Tab. 5 Ranging results under different sampling frequencies

Sampling frequency /kHz	actual fault distance /km	Ranging results /km	Ranging relative error （%）
50	150	152．1	0．70
100	150	148	0．67
250	150	151．3	0．43
500	150	149．3	0．23
1000	150	150．4	0．13

It can be seen from the ranging results in Table 5 that with the increase of sampling frequency, the relative error gradually decreases.

6 Conclusion

Aiming at the problems existing in the existing ranging methods for cable-overhead hybrid transmission lines, this paper proposes a fault location algorithm based on zero-sequence current and EMTR theory, and establishes a cable-overhead line hybrid transmission line model. First, according to the structural characteristics of the transmission line, the Karenbauer method eliminates the electromagnetic coupling between the phasors, and the current abrupt change is obtained by wavelet transform filtering. Then, the large fault section is determined by the zero-sequence current method. Then, the maximum fault current is calculated by the time reversal and superposition of the current mutation on both sides of the transmission line, and the fault location of the small fault section is carried out accurately.

The model was built on the ATPDraw platform, and the data was analyzed and processed through MATLAB software programming. The final results show that the difference of fault phase angle and transition resistance does not affect the ranging accuracy of the ranging method. When the sampling frequency is set to 1MHz, the relative error of measuring different types of faults is less than 0.57%, and the sampling frequency is inversely proportional to the relative error , the former increases and the latter decreases, which indicates that the algorithm is suitable for fault location of overhead line-cable hybrid transmission lines.

Fund Project:
The Natural Science Basic Research Program of Shaanxi Province (2021JM-393)

References

[1] Zhang Yuning.Summary of fault location methods for overhead-cable hybrid transmission lines[J].Electric Power Engineering Technology，2020，39(06):44-51.

[2] Wang Chen，Ye Jiangming，Chen Hao，et al. An improved method of one-terminal fault location for hybrid power cable-overhead line [J]. Hunan Electric Power, 2020, 40(04): 27-31.

[3] Huang Long, Xiao Xiangchun, Zeng Xiangjun，et al.Integrated fault location method for mixed lines based on traveling wave[J].Journal of Electric Power Science and Technology, 2018, 33 (01): 93-101.

[4] Xing Zhijie， Tian Xingjun， Liu Yuxi，et al. Research of traveling wave fault location algorithm for the overhead line-cable hybrid line [J].Power System Technology， 2020，44(09): 3540-3546.

[5] Wu Guoxing, Xu Shu, Li Xun. A combined traveling wave ranging method for overhead line-cable hybrid line [J]. Hydropower and Energy Science, 2017, 35(07):186-188+162.

[6] Gao Qingmin, Wei Jinmei, Chen Liping, et al. Double-ended traveling wave fault location algorithm for overhead-cable hybrid lines [J]. Journal of North China Institute of Water Conservancy and Hydropower, 2010, 31(03):55-56.

[7] Li Jun， Fan Chunju. Wavelet analysis based traveling wave fault location for hybrid transmission line consisting of power cable and overhead line[J].Power System Technology， 2006， 30(9): 92-97.

[8] Liu Shungui, Li Xun, Zhang Hongzhao, et al. A traveling wave fault location method for hybrid lines using time discrimination method [J]. Power System Protection and Control, 2017, 45(01):41-46.

[9] Song Yunhai, Wang Qi, Chang An. Distributed fault location method for overhead line-cable hybrid line [J]. Hydropower and Energy Science, 2016, 34(01):179-183.

[10] Liang Fengqiang，Chen Ping，Xu Lin，et al．A locating method through the combined traveling wave of the overhead line-submarine cable hybrid line[J].Electrical Automation，2016， 38(2): 76-79．

[11] Gaspard Lugrin， Nicolas Mora Parra， Farhad Rachidi.On the location of lightning discharges using time reversal of electromagnetic fields[J].IEEE Transactions on Electromagnetic Compatibility.2014， 56(1): 149-157.

[12] Zhang Xipeng，Tai Nengling，Zheng Xiaodong，et al.Fault location in VSC-HVDC transmission lines based on WEMTR[J].Transactions of China Electrotechnical Society，2019， 34(3): 589-598．

[13] Zhang Xipeng，Tai Nengling，Zheng Xiaodong，et al.Application basis of EMTR theory for line fault location in power system I:Theoretical Part[J].Power System Technology.2020，44(03):845-854.

[14] Zhang Xipeng， Tai Nengling， Zheng Xiaodong，et al. Application basis of EMTR theory for line fault location in power system II: Simulation Part[J].Power System Technology． 2020，44(03):854-863.

[15] Shang Liqun， Huang Ruoxuan， Hu Yanhai，et al.Fault location of double-circuit transmission lines on the same pole under different voltage levels based on electromagnetic time reversal[J].Journal of Xi'an Jiaotong University， 2020， 54(01): 19 -25+41.

[16] Shang Liqun， Hu Yanhai， Huang Ruoxuan，et al.EMTR theory-based fault location for series compensated transmission line[J].Proceedings of the Chinese Society of Electrical Engineering， 2020， 40(20): 6603-6609.

[17] Qin Siming， Li Yi.Study on the fault location method of overhead-cable-overhead hybrid lines[J].Guangxi Electric Power． 2019， 42(04)：24-28.

[18] Zhang Naigang，Zhang Jiasheng，Zheng Changming，et al. Fault section location based on similarity of zero sequence current amplitude distribution in non-solidly-earthed network[J].Power System Protection and Control,2018,46(13):120-125.

[19] Liu Siqi， Yu Kun， Zeng Xiangjun，et al. Fault location method of a non-effective earthed system based on zero sequence current amplitude continuous regulation[J].Power System Protection and Control， 2021， 49(09): 48 -56.

[20] Liao Lirong，Dong Chen，Yu Kai，et al.Application of wavelet transform in double-end fault location EHV transmission lines[J].Guangdong Electric Power， 2010， 23(11): 10-13.